Chinese Chemical Letters 37 (2026) 112084

Contents lists available at ScienceDirect

Chinese Chemical Letters

journal homepage: www.elsevier.com/locate/cclet

Acaualblides A–E, architecturally unprecedented macrolides from *Acaulium album* 429 with BCR-targeted immunosuppressive activity

Sitian Zhang[a,b,1], Qiqiang Liang[a,1], Lei Su[c,1], Xinyu Zheng[a], Hanxiao Zeng[a], Weiguang Sun[a,*], Yuan Zhou[a,*], Yonghui Zhang[a,*], Zhengxi Hu[a,d,e,*]

[a] *Hubei Key Laboratory of Natural Medicinal Chemistry and Resource Evaluation, School of Pharmacy, Tongji Medical College, Huazhong University of Science and Technology, Wuhan 430030, China*
[b] *Department of Pharmacy, Renmin Hospital of Wuhan University, Wuhan 430060, China*
[c] *NHC Key Laboratory of Human Disease Comparative Medicine, National Human Diseases Animal Model Resource Center, International Center for Technology and Innovation of Animal Model, Institute of Laboratory Animal Science, Chinese Academy of Medical Sciences (CAMS) and Peking Union Medical College (PUMC), Beijing 100021, China*
[d] *Hubei Shizhen Laboratory, Wuhan 430061, China*
[e] *School of Pharmaceutical Sciences, Zhejiang Chinese Medical University, Hangzhou 311403, China*

ARTICLE INFO

Article history:
Received 31 July 2025
Revised 5 November 2025
Accepted 6 November 2025
Available online 7 November 2025

Keywords:
Acaulium album 429
Macrolides
Acaualblides A–E
Structure elucidation
Immunosuppressive activity

ABSTRACT

Acaualblides A–E (**1**–**5**), five architecturally unprecedented macrolides, were isolated from fungus *Acaulium album* 429 and comprehensively characterized. Their structures were elucidated by high-resolution electrospray ionization mass spectrometry (HRESIMS), extensive spectroscopic analyses, and single-crystal X-ray diffraction. Compounds **1**–**3** possess unusual fourteen-membered macrolide frameworks bearing pyridine or thiophene moieties. Compound **4** represents the first heterodimer featuring a macrolide unit covalently linked to an aflatoxin B_1 moiety through a C–C bond, while compound **5** is a unique homodimeric macrolide in which two identical units are connected by both a C-9/C-9′ carbon-carbon bond and a C-8/C-8′ thioether bridge. Plausible biosynthetic pathways for compounds **1**–**5** are proposed. Notably, compound **1** displayed significant immunosuppressive activity by inhibiting B-cell proliferation and activation through modulation of the B-cell receptor (BCR) signaling pathway.

© 2026 Published by Elsevier B.V. on behalf of Chinese Chemical Society and Institute of Materia Medica, Chinese Academy of Medical Sciences.

The global incidence of autoimmune diseases continues to rise, contributing substantially to morbidity, mortality, and increasing healthcare and socioeconomic burdens, thereby posing a major public health challenge [1]. In clinical practice, immunosuppressive agents are indispensable for the management of autoimmune disorders, such as systemic lupus erythematosus and rheumatoid arthritis, as well as for the prevention of organ transplant rejection [2]. Notably, several cornerstone immunosuppressants, including rapamycin and tacrolimus, are macrolides derived from microbial secondary metabolites [3,4]. Although highly effective, their long-term use is often limited by serious adverse effects, such as nephrotoxicity, hepatotoxicity, heightened infection risk, and increased malignancy incidence [5,6], highlighting the urgent need for safer and more effective immunosuppressive agents.

Given the clinical success of macrolide scaffolds, the discovery of novel macrolides with improved safety profiles represents a promising strategy for immunosuppressant development. As part of our ongoing search for structurally unique and biologically active fungal metabolites [7,8], we examined *Acaulium album* 429, a strain isolated from chinchilla feces. Previous studies have demonstrated the ability of *A. album* to produce structurally diverse macrolides [9–11], prompting a detailed investigation of its secondary metabolites. Herein, we report the isolation, structural elucidation, proposed biosynthetic pathways, and immunosuppressive activities of five novel macrolides, acaualblides A–E (**1**–**5**), together with one known analogue (**6**) (Fig. 1).

Acaualblide A (**1**) was obtained as a colorless crystal and assigned the molecular formula $C_{18}H_{24}O_7S$ based on high-resolution electrospray ionization mass spectrometry (HRESIMS) data at *m/z* 407.1130 ($[M+Na]^+$, calcd. for $C_{18}H_{24}O_7SNa^+$, 407.1135), which indicated seven degrees of unsaturation. The ^1H nuclear magnetic resonance (NMR) spectrum of **1** displayed three doublet methyl groups at δ_H 1.27 (3H, d, $J = 6.1$ Hz), 1.39 (3H, d, $J = 6.3$ Hz), and 1.64 (3H, d, $J = 6.8$ Hz), as well as two olefinic protons at δ_H 5.80 (1H,

* Corresponding authors.
E-mail addresses: weiguang_sun@hust.edu.cn (W. Sun), yuan2273@163.com (Y. Zhou), zhangyh@mails.tjmu.edu.cn (Y. Zhang), hzx616@126.com (Z. Hu).
[1] These authors contributed equally to this work.

https://doi.org/10.1016/j.cclet.2025.112084
1001-8417/© 2026 Published by Elsevier B.V. on behalf of Chinese Chemical Society and Institute of Materia Medica, Chinese Academy of Medical Sciences.

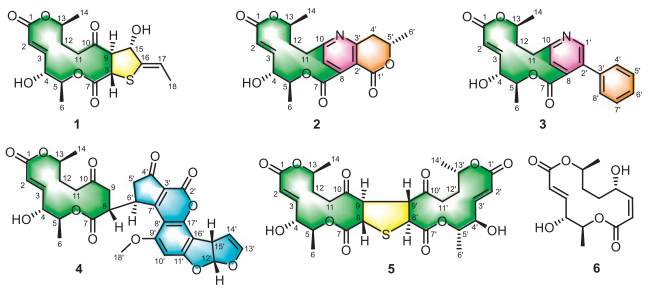


Fig. 1. Chemical structures of compounds **1**–**6**.

dd, $J = 15.8$, 1.4 Hz) and 6.63 (1H, dd, $J = 15.8$, 5.9 Hz). Together with distortionless enhancement by polarization transfer (DEPT), heteronuclear single quantum coherence (HSQC), and heteronuclear multiple bond correlation (HMBC) spectroscopy data, the ^{13}C NMR spectrum of **1** (Table S2 in Supporting information) revealed 18 carbon resonances, including three methyls, two methylenes (one oxygenated), nine methines (three olefinic and two oxygenated), one olefinic quaternary carbon, two ester carbonyls, and one ketone carbonyl, accounting for five degrees of unsaturation. Considering the molecular formula and the remaining degrees of unsaturation, compound **1** was deduced to possess a bicyclic system.

Comparison of the ^{1}H and ^{13}C NMR data of **1** with those of the known macrolide acaulone A [9] suggested the presence of a 14-membered macrolide framework. This was further supported by the ^{1}H–^{1}H COSY correlations of H-2/H-3/H-4/H-5/H_3–6, H-8/H-9/H-15, H_2–11/H_2–12/H-13/H_3–14, and H-17/H_3–18, as well as the HMBC correlations (Fig. S2 in Supporting information) from H-3 to C-1, C-2, and C-4, from H-4 to C-5, from H_3–6 to C-5, from H-9 to C-7, C-8, and C-10, from H_3–14 to C-12 and C-13. Additional HMBC correlations from H-15 (δ_H 4.37) to C-9 (δ_C 62.1), C-16 (δ_C 139.8), and from H-17 (δ_H 5.62) to C-15 (δ_C 80.1), C-16, C-18 (δ_C 15.3), together with the key nuclear Overhauser enhancement spectroscopy (NOESY) correlation between H-8 (δ_H 4.25) and H-15, indicated that a 2-ethylidenetetrahydrothiophen-3-ol moiety was fused to 14-membered macrolide *via* the C-8–C-9 bond. Thus, the planar structure of **1** was established.

The relative configuration of **1** was further investigated by detailed analysis of the NOESY spectrum. However, due to the conformational flexibility of the macrodilactone, the stereochemistry at C-4, C-5, C-8, and C-13 could not be resolved unambiguously. Fortunately, a high-quality crystal of **1** was obtained by repeated recrystallization and subjected to single-crystal X-ray diffraction analysis using Cu Kα radiation (Fig. 2) [Flack parameter = 0.001(6), CCDC 2393816], which not only confirmed the planar structure but also established the absolute stereochemistry of **1** as 4*R*,5*S*,8*S*,9*R*,13*S*,15*S*,$\Delta^{2,3}$*E*,$\Delta^{16,17}$*Z*. Accordingly, the absolute structure of **1** was determined.

Acaualblide B (**2**) was isolated as a colorless crystal, and its molecular formula was determined as $C_{20}H_{23}NO_7$, on the basis of its HRESIMS data at *m/z* 412.1317 $[M+Na]^+$ (calcd. for $C_{20}H_{23}NO_7Na^+$, 412.1367), which suggested ten degrees of unsaturation. The ^{13}C NMR spectrum (Table S2), analyzed with the aid of DEPT and HSQC experiments, revealed 20 carbon resonances. Comparison of the ^{1}H and ^{13}C NMR data (Table S2) of **2** with those of **1** suggested that both compounds shared a 14-membered macrolide framework. Among these data, four double bonds and three ester carbonyls accounted for seven of the ten indices of hydrogen deficiency, suggesting that **2** was a rare 14-membered macrolide derivative containing three ring systems.

The proton-proton correlation spectroscopy (^{1}H–^{1}H COSY) correlations (Fig. S2) of H_2–4′/H-5′/H_3–6′, together with the HMBC correlations (Fig. S2) from H_2–4′ (δ_H 3.06/3.16) to C-1′ (δ_C 163.1), C-3′ (δ_C 159.4), C-5′ (δ_C 74.9), and C-6′ (δ_C 20.9), and from H-9 (δ_H 6.90) to C-1′, established the presence of a 3,4-disubstituted 6-methyl-2-pyrone motif. Detailed analysis of the 2D NMR spectra revealed a high degree of structural similarity between compound **2** and acatulide A [11]. The distinction was clarified by the unsaturation index and molecular weight, which indicated that the two motifs in **2** were connected through a C-10–N–C-3′ linkage, in contrast to the C-10–O–C-3′ connection observed in acatulide A.

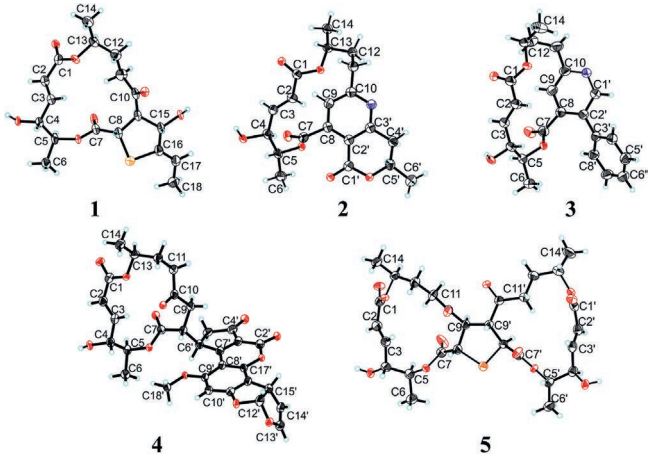


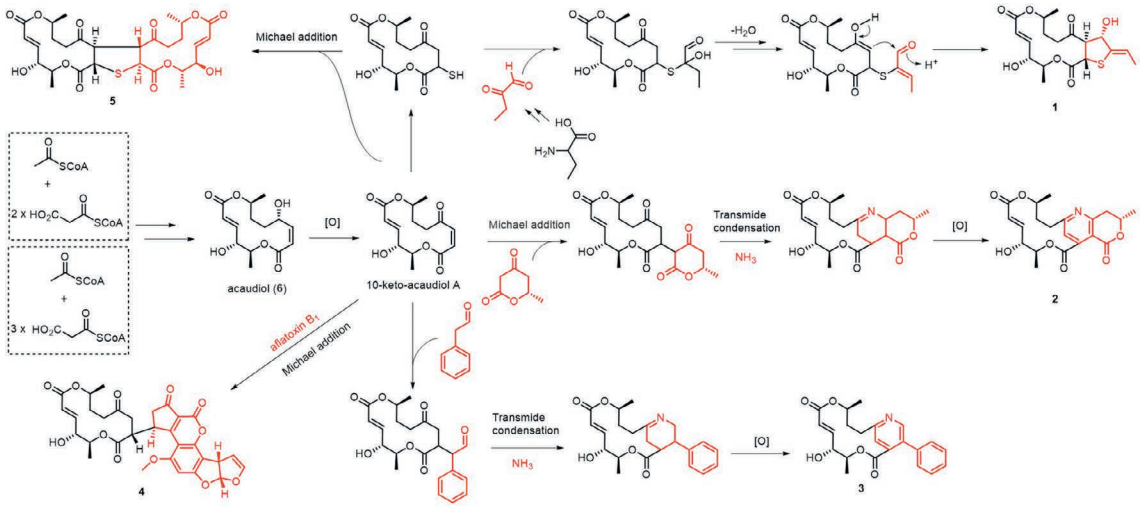
Fig. 2. X-ray Oak Ridge thermal ellipsoid plot (ORTEP) drawings of compounds of **1**–**5**.

In view of their common biosynthetic origin, the configuration of **2** was deduced to be identical to that of **1**, except for C-5′. However, the relative configuration of C-5′ in **2** could not be resolved by NOESY experiment. Fortunately, repeated recrystallization afforded a suitable crystal of **2**, which was subjected to single-crystal X-ray diffraction using Cu Kα radiation (Fig. 2) [Flack parameter = 0.08(10), CCDC 2393818]. This analysis not only corroborated the planar structure but also established the absolute configuration of **2** as 4*R*,5*S*,13*S*,5′*S*,$\Delta^{2,3}$*E*. Accordingly, the absolute structure of **2** was defined.

Acaualblide C (**3**) had the molecular formula $C_{22}H_{23}NO_5$, as deduced from HRESIMS data, which indicated twelve degrees of unsaturation. Comprehensive analysis of the NMR data (Table S2) revealed that **3** was a structural congener of **2**. Excluding the signals attributable to the macrodilactone moiety, the residual signals suggested the presence of a monosubstituted benzene ring. This assumption was further confirmed by the key ^{1}H–^{1}H COSY correlation of H-4′/H-5′/H-6′/H-7′/H-8′, along with the HMBC correlations from H-5′/7′ (δ_H 7.46) to C-3′ (δ_C 138.1) and from H-4′/8′ (δ_H 7.41) to C-2′ (δ_C 134.0). In addition, a pyridine unit was fused to the macrodilactone *via* C-8/C-9/C-10, as supported by the HRESIMS data, the degrees of unsaturation, and the HMBC correlations (Fig. S2) from H-9 (δ_H 7.14) to C-7 (δ_C 169.3), C-10 (δ_C 162.6), C-11 (δ_C 36.8), and C-2′, as well as from H-1′ (δ_H 8.59) to C-2′, C-8 (δ_C 141.9), and C-10. On this basis, the planar structure of **3** was elucidated as shown in Fig. 1.

Given their shared biosynthetic origin, **3** was proposed to have the same configurations at C-4, C-5, and C-13 as those of **2**. After repeated recrystallization from MeOH–H_2O (20:1), a high-quality crystal of **3** was obtained and then subjected to single-crystal X-ray diffraction analysis using Cu Kα radiation (Fig. 2) [Flack parameter = 0.08(7), CCDC 2393817], which not only confirmed its planar structure but also suggested the absolute stereochemistry of **3** to be 4*R*,5*S*,13*S*,$\Delta^{2,3}$*E*.

Acaualblide D (**4**) was isolated as a colorless crystal, and its molecular formula was determined as $C_{31}H_{30}O_{12}$ from ^{13}C NMR and HRESIMS data, which indicated 17 degrees of unsaturation. De-



Scheme 1. Plausible biosynthetic pathways for compounds **1**–**5**.

tailed comparison of the 1D NMR data (Table S3 in Supporting information) of **4** with those of 10-keto-acaudiol A [7], together with 2D NMR analyses, revealed the presence of a 14-membered macrocyclic fragment. Subtraction of the 14 carbons comprising the macrocyclic diester framework from the molecular formula left a residual substructure of 17 carbons with 12 degrees of unsaturation. This pattern corresponded to an aflatoxin-derived fragment, as supported by diagnostic HSQC, HMBC, and ^{1}H–^{1}H COSY correlations. The ^{1}H–^{1}H COSY cross-peaks of H_2–9/H-8/H-6′/H_2–5′, along with the HMBC correlations from H-6′ to C-9, C-3′, C-4′, and C-5′, and from H-8 to C-9 and C-7 (Fig. S2), established that the two fragments were connected through a C-8–C-6′ bond, thereby defining the planar structure of **4**.

The relative conformations of C-4, C-5, C-8, and C-13 could not be determined by the NOESY spectrum because of the conformational flexibility of the macrolide moiety and partial signal overlap. Fortunately, a high-quality crystal of **4** was obtained after repeated recrystallization from the MeOH–CH_2Cl_2 system and subjected to single-crystal X-ray diffraction analysis with Cu Kα radiation (Fig. 2) [Flack parameter = 0.07(9), CCDC 2452329]. Thus, the absolute stereochemistry of **4** was determined to be 4*R*,5*S*,8*R*,13*S*,6′*R*,12′*R*,15′*S*,$\Delta^{2,3}$*E*.

Acaualblide E (**5**) was obtained as a colorless crystal, and its molecular formula was determined as $C_{28}H_{36}O_{12}S$ based on the ^{13}C NMR and HRESIMS data, corresponding to 11 degrees of unsaturation. Detailed analysis of the 1D NMR spectra (Table S3) revealed characteristic features of a 14-membered macrolide scaffold. Further comprehensive interpretation of the 2D NMR data, supported by mass spectrometric evidence, revealed that compound **5** possessed a centrosymmetric 14-membered macrocyclic lactone dimer framework.

The monomeric unit accounted for five degrees of unsaturation; thus, the observed total of 11 degrees of unsaturation suggested the formation of a fused structure involving two identical monomers. Moreover, the presence of hypomethyl-type carbon resonances at C-8 and C-9 indicated the construction of a thiophene-embedded pentacyclic system through a direct C–C bond and a C–S–C thioether linkage between the two monomeric units. However, owing to the conformational flexibility of the macrolide ring, critical NOE correlations required for defining its spatial configuration were not observed.

Fortunately, a suitable crystal of **5** was obtained by slow recrystallization from MeOH–H_2O (100:1), and its absolute configuration was unambiguously confirmed by single-crystal X-ray diffraction analysis using Cu Kα radiation (Fig. 2; Flack parameter = 0.05(11); CCDC 2452330). The absolute stereochemistry was thus assigned as 4/4′*R*,5/5′*S*,8/8′*S*,9/9′*R*,13/13′*S*,$\Delta^{2,3}/\Delta^{2',3'}$*E*.

The plausible biosynthetic pathways of compounds **1**–**5** were proposed in Scheme 1. Based on previously reported biosynthetic mechanisms of related macrocyclic lactones [11], compound **6** (acaudiol) was hypothesized to be derived *via* Claisen-type decarboxylation and subsequent lactonization of an acetyl starter unit extended by two or three malonyl-derived building blocks. Oxidation at the C-10 hydroxyl position of compound **6** appeared to be a critical step that contributed to the structural diversification of fungal macrocyclic lactones. The sulfated derivative of 10-ketoacaudiol was proposed to have undergone nucleophilic addition, dehydration, and aldol condensation with 2-oxobutanal derived from 2-aminobutanoic acid to generate acaualblide A (**1**). Acaualblide B (**2**) was proposed to be formed through a sequence involving Michael addition, transamination, condensation, and oxidation between 10-keto-acaudiol A and (*S*)-6-methyldihydro-2*H*-pyran-2,4(3*H*)–dione. Likewise, acaualblide C (**3**) was proposed to have been biosynthesized from 10-ketoacaudiol and 2-phenylacetaldehyde *via* transmide condensation followed by oxidative modification. Acaualblide D (**4**) was likely generated through a Michael addition between 10-ketoacaudiol and a fragment derived from aflatoxin B_1. In the case of acaualblide E (**5**), a dimerization event involving 10-ketoacaudiol and its vulcanized (sulfur-bridged) derivative was proposed to afford the final thiophene-containing macrocyclic dimer.

Autoimmune diseases arise from abnormal immune system activation and involve complex pathogenesis influenced by genetic, environmental, and other factors. Despite advancements in therapeutic interventions, substantial challenges remained [12]. Natural products have shown considerable potential for immunomodulatory drug development. Accordingly, we evaluated the immunosuppressive activity of this series of compounds. As shown in Fig. S1 (Supporting information), compound **1** exhibited no significant cytotoxicity at the tested concentrations, yet it markedly inhibited LPS-induced B lymphocyte proliferation. With the half maximal inhibitory concentration (IC_{50}) value of 3.27 ± 0.15 μmol/L, compound **1** outperformed compound **5** but was slightly less potent than cyclosporine (Cyclosporine capsules).

Lipopolysaccharide (LPS) activates the Toll-like receptor 4 (TLR4) signaling pathway and promotes B cells to secrete pro-inflammatory cytokines, including tumor necrosis factor-alpha (TNF-α), interleukin-6 (IL-6), and interferon-gamma (IFN-γ)

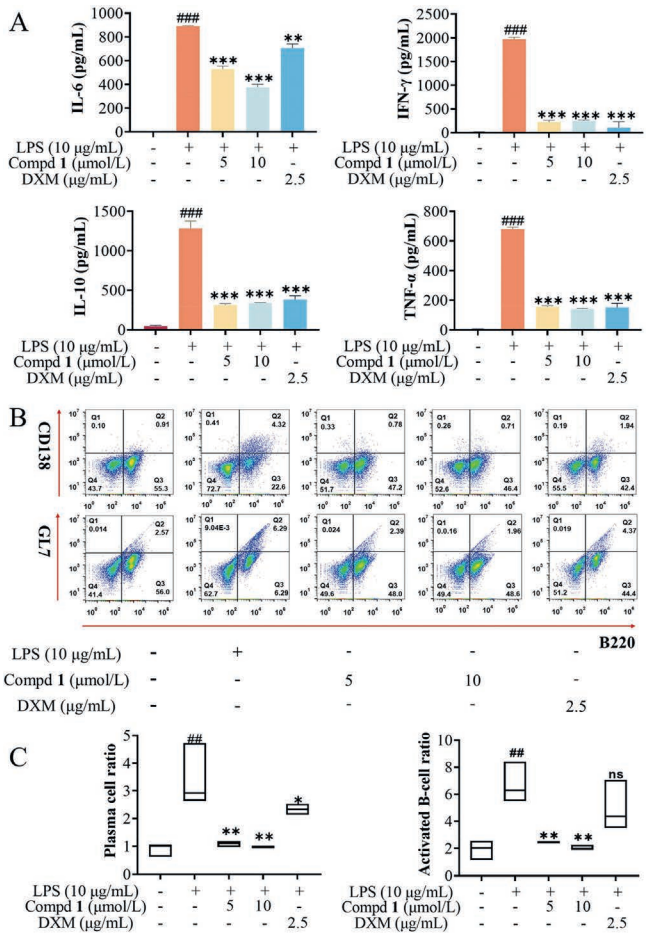


Fig. 3. Effects of compound **1** on LPS-induced abnormal proliferation and differentiation of B lymphocytes, as well as inflammatory cytokine production. (A) Compound **1** markedly suppressed LPS-induced cytokine release. (B, C) Inhibitory effects of compound **1** on $GL7^+$ activated B cells and $CD138^+$ plasma cells. Data are presented as mean ± standard deviation (SD) ($n = 3$). Statistical significance was determined by ordinary one-way ANOVA. $^{\#\#}P < 0.01$, $^{\#\#\#}P < 0.001$ *vs.* control group; $^{*}P < 0.05$, $^{**}P < 0.01$, $^{***}P < 0.001$ *vs.* LPS-treated group. ns, not significant.

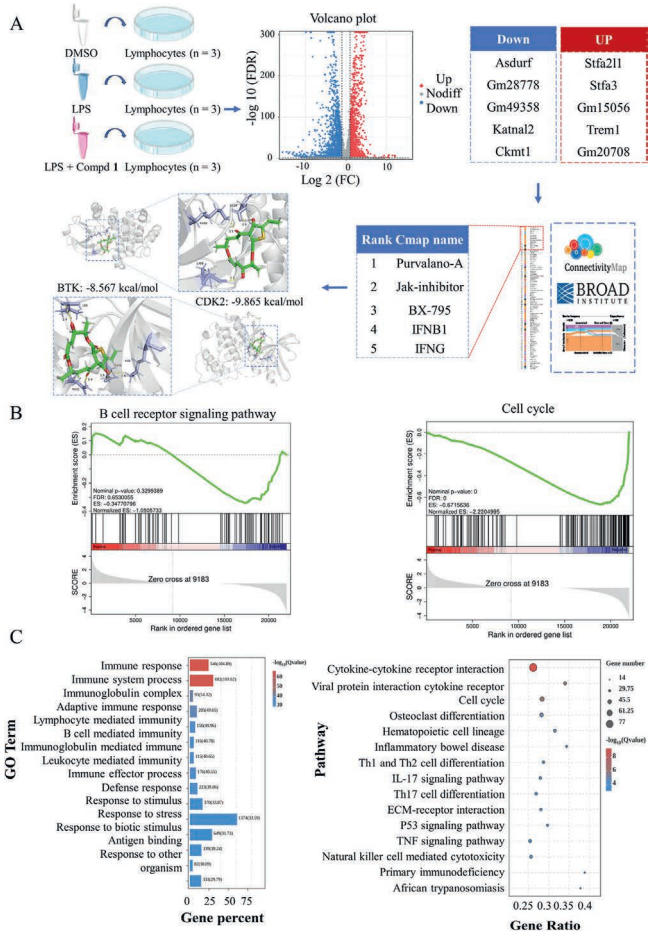


Fig. 4. Transcriptomic analysis of compound **1**. (A) Molecular docking simulation based on transcriptomic data of compound **1** analyzed *via* the CMAP database. (B) GSEA of the BCR signaling pathway and cell cycle signaling pathway. (C) GO and KEGG pathway enrichment analyses.

[13–16]. These cytokines play pivotal roles in driving B cell proliferation, differentiation, and immune amplification. In our study, LPS stimulation significantly increased the secretion of TNF-α, IL-6, IFN-γ, and IL-10 by B cells. Compared with the LPS group, compound **1** significantly inhibited cytokine secretion at the tested concentrations (Fig. 3A). Furthermore, flow cytometric analysis revealed that LPS treatment elevated the proportions of $GL7^+$ activated B cells and $CD138^+$ plasma cells relative to the control group. Treatment with compound **1** markedly reduced these populations, indicating its inhibitory effect on LPS-induced B cell activation and differentiation (Figs. 3B and C).

To investigate the molecular targets and signaling pathways affected by compound **1**, transcriptomic (RNA-seq) analysis was performed to profile global gene expression changes in B lymphocytes under different treatments. The connectivity map (CMAP) database, a powerful tool for elucidating drug mechanisms and natural product research [17], was employed to analyze gene expression data from B cells treated with compound **1**. A total of 218 differentially expressed genes (fold change ≥ 1.2, $P < 0.001$), including 110 upregulated and 108 downregulated genes, were submitted as query signatures (Fig. 4A).

CMAP analysis revealed that compound **1** exhibited the strongest positive correlations with inhibitors of cyclin-dependent kinases (CDKs), Janus kinases (JAKs), and inhibitor of kappa B kinases (IKKs). Gene ontology (GO) and Kyoto encyclopedia of genes and genomes (KEGG) pathway enrichment analyses indicated that these genes were primarily involved in immune system processes, T helper 1 (Th1) and Th2 cell differentiation, and inflammatory bowel disease. Among the 15 significantly downregulated KEGG pathways, the B-cell receptor (BCR) and cell cycle pathways were highly enriched and closely interconnected, suggesting that they may mediate the effects of compound **1** on B cells. Previous studies have implicated these pathways in B cell proliferation and activation [18].

Gene set enrichment analysis (GSEA) further confirmed the downregulation of the BCR signaling pathway in the compound **1**-treated group, with core genes such as SYK, BTK, and PLCγ showing decreased expression. Similarly, cell cycle-related genes, including various cyclins and CDKs, were significantly suppressed, as reflected in the GSEA enrichment plots. Based on these findings, we proposed that compound **1** inhibited B cell proliferation and differentiation by targeting the BCR and cell cycle signaling pathways. Supporting this hypothesis, molecular docking simulations demonstrated that compound **1** bound with high affinity to CDK2 and Bruton's tyrosine kinase (BTK), key regulators of the cell cycle and BCR pathways, respectively (Figs. 4B and C).

To further elucidate the mechanism of action of compound **1**, Western blot analysis was performed, revealing that compound **1** markedly reduced the phosphorylation levels of BTK, SYK, and protein kinase B (AKT). Additionally, quantitative mRNA analysis

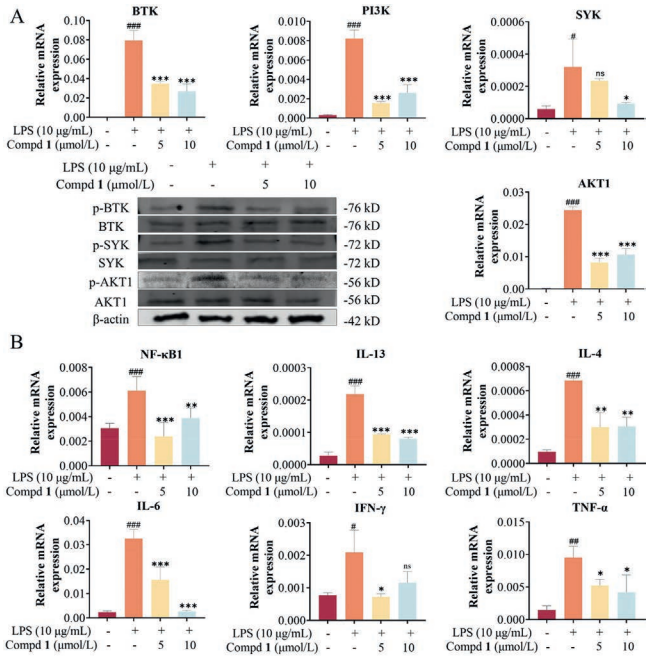


Fig. 5. Effects of compound **1** on the BCR signaling pathway. (A) Compound **1** reduces the phosphorylation levels and mRNA expression levels of key molecules in the B cell receptor signaling pathway. (B) mRNA expression levels of downstream immune factors in the B cell receptor signaling pathway. Data are presented as mean ± SD ($n = 3$). Statistical significance was determined by ordinary one-way ANOVA. $^{\#}P < 0.05$, $^{\#\#}P < 0.01$, $^{\#\#\#}P < 0.001$ *vs.* control group; $^{*}P < 0.05$, $^{**}P < 0.01$, $^{***}P < 0.001$ *vs.* LPS group.

showed that compound **1** significantly decreased the expression of key BCR pathway molecules (BTK, SYK, AKT, phosphoinositide 3-kinase (PI3K), *etc.*) and downstream immune factors (Figs. 5A and B). Collectively, these findings suggest that compound **1** exerts immunosuppressive effects by modulating the BCR–cell cycle signaling pathway, providing a mechanistic basis for further investigation of its key regulatory targets.

In summary, five skeletally unprecedented macrolides, acaublides A-E (**1**–**5**), were isolated from the solid-state culture of *Acaulium album* 429 derived from chinchilla feces. Their structures were elucidated by comprehensive spectroscopic analyses, including HRESIMS, NMR, and single-crystal X-ray diffraction (Cu Kα). Compounds **1**–**3** possess unusual fourteen-membered macrolide frameworks bearing pyridine or thiophene moieties. Compound **4** represents the first heterodimer linked *via* a C–C bond to an aflatoxin B_1 fragment, while compound **5** is a homodimer featuring both a C-9/C-9′ carbon-carbon bond and a C-8/C-8′ thioether bridge. Bioactivity assays revealed that compound **1** exhibited notable immunosuppressive activity by inhibiting B-cell proliferation and activation, through modulation of the BCR signaling pathway. These findings enrich the structural diversity of fungal macrolides and highlight their potential as scaffolds for immunosuppressive drug discovery and biosynthetic studies.

CRediT authorship contribution statement

Sitian Zhang: Investigation. **Qiqiang Liang:** Investigation. **Lei Su:** Resources. **Xinyu Zheng:** Investigation. **Hanxiao Zeng:** Formal analysis. **Weiguang Sun:** Validation, Supervision. **Yuan Zhou:** Validation. **Yonghui Zhang:** Writing – review & editing, Funding acquisition. **Zhengxi Hu:** Writing – review & editing, Validation.

Declaration of competing interest

The authors declare that they have no known competing financial interests or personal relationships that could have appeared to influence the work reported in this paper.

Acknowledgments

We thank the Analytical and Testing Center at Huazhong University of Science and Technology (HUST) for measuring ECD, IR, UV and single-crystal X-ray diffraction data. Thanks also for the technical support by the Medical Subcenter of HUST Analytical & Testing Center. This project was financially supported by the National Program for Support of Top-notch Young Professionals (No. 0106514050), the Hubei Provincial Natural Science Foundation of China (No. 2024AFA028), and the National Natural Science Foundation of China (Nos. 82273811, 22577033, 82173705, and U22A20380), the Fundamental Research Funds for the Central Universities (No. 2025BRA015), the National Key Research and Development Program of China (No. 2021YFA0910500), and the Nonprofit Central Research Institute Fund of Chinese Academy of Medical Sciences (No. 2023-PT180–01).

Supplementary materials

Supplementary material associated with this article can be found, in the online version, at doi:10.1016/j.cclet.2025.112084.

References

[1] F.W. Miller, Curr. Opin. Immunol. 80 (2023) 102266.
[2] J. Walczak, D. Iwaszkiewicz-Grześ, G. Cholewiński, Curr. Top. Med. Chem. 24 (2024) 1230–1263.
[3] B.M. Shrestha, Exp. Clin. Transplant. 15 (2017) 1–9.
[4] A. Mika, P. Stepnowski, J. Pharm. Biomed. Anal. 127 (2016) 207–231.
[5] M.D. Stegall, R.E. Morris, R.R. Alloway, et al., Am. J. Transplant. 16 (2016) 1094–1101.
[6] T.R. Srinivas, H.U. Meier-Kriesche, Clin. J. Am. Soc. Nephrol. 2 (2008) S101–S116.
[7] M. Zheng, Y. Liu, C. Chen, et al., Chin. Chem. Lett. 36 (2025) 110904.
[8] Z. Shi, J. Yin, Y. Xiao, et al., Chin. Chem. Lett. 35 (2024) 109458.
[9] T.T. Wang, Y.J. Wei, H.M. Ge, et al., Org. Lett. 20 (2018) 1007–1010.
[10] Z.W. Tong, X.H. Xie, T.T. Wang, et al., Org. Lett. 23 (2021) 5587–5591.
[11] Z.W. Tong, T.T. Wang, P. Yang, et al., Chin. Chem. Lett. 35 (2024) 108488.
[12] J.S. Smolen, D. Aletaha, I.B. McInnes, Lancet 388 (2016) 2023–2038.
[13] E.L. Carpenter, R. Mick, J. Rüter, et al., J. Transl. Med. 7 (2009) 93.
[14] S.X. Ye, Q.Y. Zheng, Y. Zhou, et al., Molecules 24 (2019) 3731.
[15] S. Agrawal, S. Gollapudi, H. Su, et al., J. Clin. Immunol. 31 (2011) 472–478.
[16] S. Cheng, H. Wang, H. Zhou, J. Immunol. Res. 2016 (2016) 1719720.
[17] O. Ernst, Y. Glucksam-Galnoy, M. Athamna, et al., Mediators Inflamm. 2019 (2019) 3451461.
[18] S. Richards, C. Watanabe, L. Santos, et al., Immunol. Rev. 224 (2008) 183–200.